RESILIENT INFRASTRUCTURE
June 1–4, 2016
RESILIENT INFRASTRUCTURE LONDON 2016

NUMERICAL MODELLING OF REINFORCED CONCRETE BLOCK STRUCTURAL WALL BUILDINGS UNDER SEISMIC LOADING

Mohamed Ezzeldin
Ph.D. Candidate, McMaster University, Canada

Lydell Wiebe
Assistant Professor, McMaster University, Canada

Wael El-Dakhakhni
Martini, Mascarin and George Chair in Masonry Design, McMaster University, Canada

ABSTRACT

With the recent shift of design code developers' focus from component- to system-level assessment of seismic force resisting systems, there is a need to numerically assess the performance of whole buildings. However, reinforced concrete block structural wall buildings are complex structural systems composed of materials with nonlinear and heterogeneous properties, which makes the numerical investigation challenging, especially when seismic behavior is considered. Most previous numerical models of reinforced concrete block walls have considered individual components, rather than the complete building system, and have used relatively complex micro-models. In this paper, OpenSees (Open System for Earthquake Engineering Simulation) is used to create macro non-linear models to simulate the response of two different buildings under unidirectional cyclic loading that represents earthquake effects. The models are created in such a way as to balance the desire for accuracy with the desire for relatively simple models that can be defined using only the geometry and actual material properties, and that are not excessively demanding computationally. Detailed validation of the models is conducted to compare the hysteretic behaviour of the numerical models with available experimental test results on reinforced concrete block structural wall buildings. This paper demonstrates that simple models can, with proper calibration, capture the cyclic response, including energy dissipation and degradation of strength, very well. In this way, this study significantly enhances the database of validated numerical models for reinforced masonry shear wall buildings.

Keywords: Seismic Analysis, Nonlinear Models, OpenSees, Reinforced Masonry, System-Level Behaviour.

1. INTRODUCTION

Fully grouted reinforced masonry (RM) shear walls have been widely used as the main lateral load resistance systems within buildings because of their inherently large lateral stiffness and lateral load resistance. The behaviour of these walls depends on the behaviour of several materials that have different characteristics (e.g. blocks, reinforcement, grout), making the nonlinear analysis of such walls challenging. Many previous studies have been conducted to numerically simulate the nonlinear behaviour of RM shear walls considering the individual components, rather than the complete building system. However, many researchers argued that there are some system-level aspects (e.g. slab's in-plane and out-of-plane rigidity) that cannot be evaluated or assessed through component-level studies. For example, Ashour et al. (2015) reported that slab flexural coupling was an important system-level aspect that affected the overall RM building performance. This included the building stiffness, lateral resistance capacity, and trend of stiffness degradation, which in turn would significantly change the overall building response under seismic loading. Consequently, there is a need to numerically quantify the performance of whole RM buildings using simple models. This paper develops a three-dimensional (3D) numerical model in OpenSees to simulate the behaviour of RM shear wall buildings under cyclic loading. A description of the experimental programs used to validate the proposed modelling technique is presented, followed by a detailed description of the 3D model. The model is then validated against the experimental results.

2. BACKGROUND ON NUMERICAL MODELS OF RM SHEAR WALLS

Many studies have been conducted to simulate the nonlinear behaviour of individual RM components, when compared to those on RM walls at the system-level. These studies can be categorized under two levels of refinement: 1) micro-modelling, where each component of the masonry wall is modelled individually, and 2) macro-modelling, where an equivalent material is used to model the masonry wall as a larger unit.

2.1 Micro-Modelling

Micro-modelling is a well-known approach for small structures. In a micro model, the structure is discretized into a finite number of small elements interconnected at a finite number of nodes. The main elements used in this kind of modelling are masonry, mortar joint, masonry-mortar interface and steel elements. Since each element can be modelled in detail, a micro-modelling strategy is often preferred for understanding the local behaviour of masonry failures for small structural elements (e.g. assemblages). Modern plasticity concepts have been used to develop an interface cap model, capable of capturing masonry failure mechanisms, including tensile cracking, frictional slip and crushing along interfaces (Lourenço et al. 1997). This approach was extended to study the individual fracture of mortar and bricks (Guinea et al. 2000).

Although micro-modelling can produce very accurate results, it is computationally expensive because the relatively small dimensions of the elements require a large number of nodes. Therefore, it may not be practical for modelling complete masonry buildings.

2.2 Macro-Modelling

Macro-modelling is based on representing the structure with a small number of elements, each of which has properties that are equivalent to the sum of its components. It is commonly used for large structures to study properties such as energy dissipation, structure deformation and strength capacity. This method does not require the level of detailed representation used for micro-modelling, so it is more practical for numerical modelling of complete masonry buildings. Legeron et al. (2005) used a finite element analysis based on multilayer elements with damage mechanics to model monotonically and cyclically loaded reinforced concrete structures. In order to capture the different failure modes of masonry-infilled RC frames, Stavridis and Shing (2010) considered a combination of the smeared and discrete crack approaches to capture all the failure modes of masonry infilled reinforced concrete structures.

Both of these models needs a high level of detail, which results in a high level of computational effort. Therefore, there is still a need to develop more simplified models based on material and geometrical properties, which can simulate the behaviour of reinforced masonry buildings.

3. EXPERIMENTAL PROGRAMS

In this paper, the numerical models of RM shear wall buildings are validated against the experimental results of Heerema et al. (2015) and Ezzeldin et al. (2016). These previous experimental programs were selected because they include walls with different level of coupling and different wall configurations with a range of aspect ratios, from 1.5 to 4.6. More details regarding the experimental programs are given in this section.

3.1 Buildings Layout

Heerema et al. (2015) tested a one-third scaled two-story asymmetrical RM shear wall building (referred to as *Building II*) under displacement-controlled quasi-static cyclic fully-reversed loading. However, the level of coupling between walls during the test was minimized in order to isolate and quantify the torsional response of the building. This was done by detailing the building with hinge lines along the two floor slabs, in order to prevent coupling and to facilitate in-plane diaphragm rotation and subsequent building twist. *Building II* was composed of four traditional shear walls aligned along the loading direction, and four other orthogonal rectangular shear walls, as shown in Figure 1a. The overall height of the building was 2,160 mm, comprised of two floors, each 1,000 mm in height, corresponding to 3,000 mm in full-scale, with slotted 80 mm thick reinforced concrete (RC) floors, each 2,400 mm

× 2,400 mm in plan. The building was fixed to the laboratory structural floor by 16 prestressed anchors through a square RC foundation (3,000 mm × 3,000 mm) with a thickness of 250 mm.

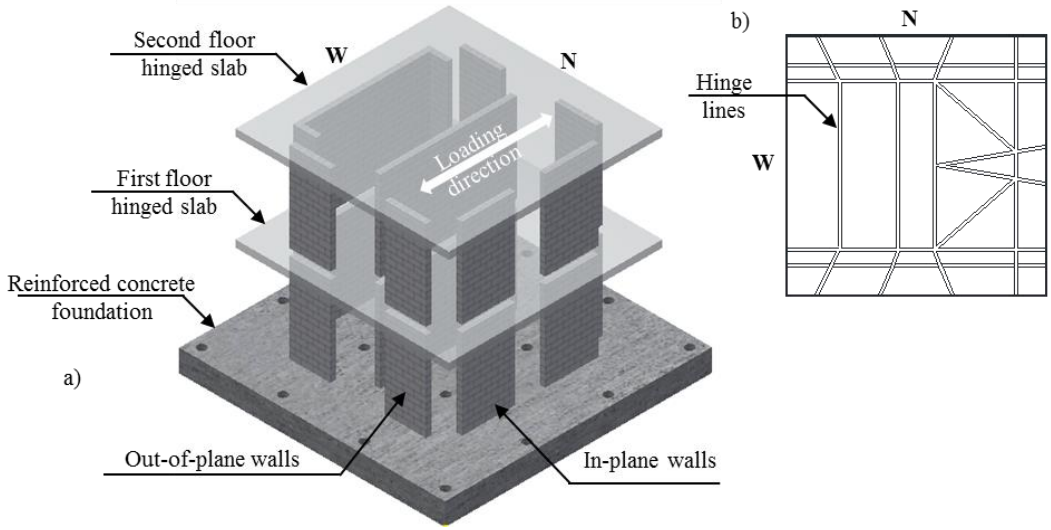

Figure 1: *Building II* configuration; a) Isometric view from East-South direction; b) RC slab detailed with hinge lines.

Ezzeldin et al. (2016) tested a nominally identical building (referred to as *Building IV*), but without hinge lines, in order to investigate the effects of wall coupling on the building and wall response. In addition, the traditional RM shear walls located along the main direction of loading in *Building II* were replaced with confined RM shear walls with boundary elements in *Building IV*, as shown in Figure 2. The boundary elements were adopted in *Building IV* because they allow closed ties to be used and multiple layers of vertical bars to be accommodated, thus providing a confining reinforcement cage. This enhances the overall performance of the RM wall relative to traditional rectangular RM wall systems, which typically have single-leg horizontal reinforcement and a single layer of vertical reinforcement because of practical limitations associated with concrete masonry unit geometrical configuration and construction techniques.

The wall configuration in plan for both buildings was selected in order to produce an eccentricity between the building floor Center of Mass, C_M, and the building Center of Rigidity, C_R, at the roof level, so as to engage the torsional response of the building under the applied lateral loads. Full details of the experimental programs and test results can be found in Heerema et al. (2015) and Ezzeldin et al. (2016) for *Building II* and *Building IV*, respectively.

3.2 Materials

A one-third scale version of the standard two-cell 190-mm hollow concrete masonry unit (190 × 190 × 390 mm) commonly used in North America was used for both buildings' wall construction. The reduced-scale concrete blocks were 130 mm in length, 63 mm in width and 63 mm in height. Table 1 summarizes the average compressive strength of the prisms, f'_m, and the average yield strengths of the vertical and the horizontal bars, f_{yv} and f_{yh}, respectively, within *Building II* and *Building IV*.

Table 1: Summary of material properties within *Building II* and *Building IV*.

Building	f'_m (MPa)	f_{yv} (MPa)	f_{yh} (MPa)
Building II	18.2	489	498
Building IV	17.9	457	487

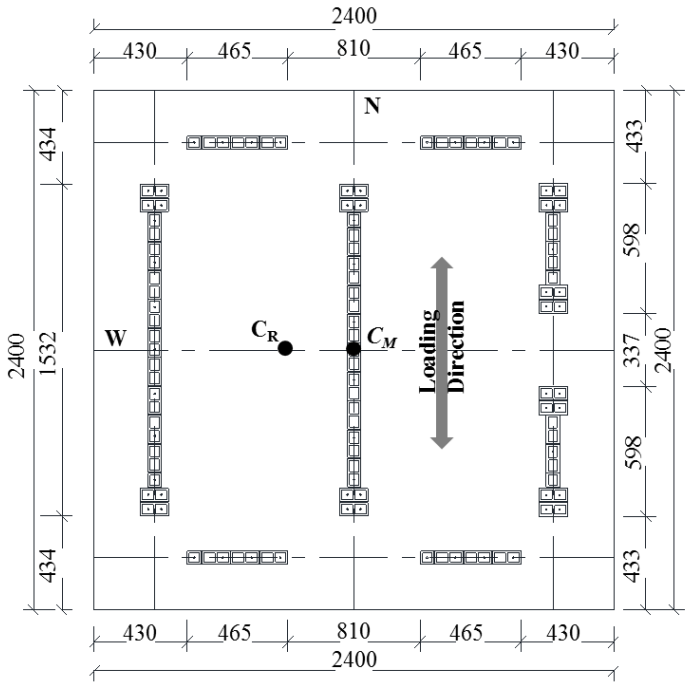

Figure 2: Plan of *Building IV*.

3.3 Test Protocol

The cyclic loading scheme for both buildings consisted of a series of displacement-controlled loading cycles to assess the strength and the stiffness degradation. The lateral cyclic displacement was applied using a hydraulic actuator, with a maximum capacity of 500 kN and a maximum cyclic stroke of 250 mm in both directions. To obtain information that included the post-peak behaviour, the displacements were increased beyond when the building had reached its maximum lateral load resistance, until the building resistance reduced to approximately 80% of its maximum capacity.

4. NUMERICAL MODEL

4.1 Selection of Elements

In this paper, a three-dimensional (3D) model was developed using OpenSees (McKenna et al. 2013) to simulate the inelastic behaviour of *Building II* and *Building IV* under cyclic loading. Displacement-based beam-column elements were adopted to model the walls of both buildings. Displacement-based beam-column elements follow the standard finite element formulation, in which the element displacement field is derived from nodal displacements. The formulation of this element assumes a linear curvature distribution and a constant axial strain. The beam-column elements were assigned fiber sections that discretely modelled the reinforcement and masonry regions. The choice of element length is a very important aspect when displacement-based beam-column elements are used with distributed plasticity and strain-softening material laws. This is because of strain localization, in which the plastic deformation tends to concentrate in the first element above the base of the wall, while the adjacent elements remain elastic (Coleman and Spacone 2001, Ezzeldin et al. 2014). Because of strain localization, the numerical results are very sensitive to the length of the first element length above the base, which should be equal to the plastic hinge length. The formula proposed by Bohl and Adebar (2011) was found to give a good estimate of the plastic hinge length for RM shear walls with and without boundary elements (Ezzeldin et al. 2015). Figure 3a shows a schematic diagram of the modelling technique used for the RM walls within the 3D model for both buildings, including the distribution of nodes and elements.

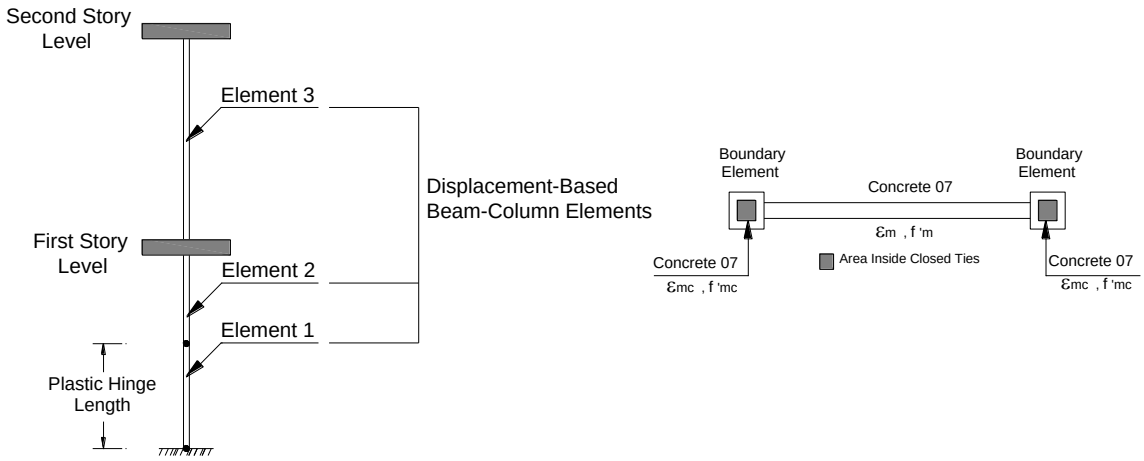

Figure 3: Schematic diagram of the modelling technique used for RM walls within the 3D model; (a) Schematic diagram in elevation of RM walls; (b) Material distribution of RM walls with boundary elements (Ezzeldin et al. 2015)

The two RC floor slabs of *Building II* were detailed with hinge lines to prevent the coupling between the RM walls and to facilitate in-plane diaphragm rotation and subsequent building twist. As such, the floor slabs in *Building II* were modelled considering the diaphragm to have no out-of-plane stiffness, while being rigid in plane, such that the nodal displacements can be expressed by two horizontal translations and one rotation about the normal to the floor-plane.

In *Building IV*, the slabs were not detailed with hinge lines, so they were simulated using multi-layer shell elements (ShellMITC4 in OpenSees). The multi-layer shell element is based on the principles of composite material mechanics. It is made up of a number of layers with specified thicknesses and material properties. The strains and curvatures of the middle-layer of the shell element are firstly obtained during the computation, and the strains in other layers can be determined based on the "plane-in-plane" assumption (Lu et al. 2015). Each RC slab in *Building IV* at each floor was modelled using 80 ShellMITC4 elements. The 80 mm thickness of the slab was defined by 8 concrete layers. The slab reinforcement was modelled using 4 layers to represent the upper and lower rebars in the two directions. Figure 4 shows a schematic diagram of the modelling technique used within the 3D model for *Building IV*, including the distribution of shells and beam-column elements.

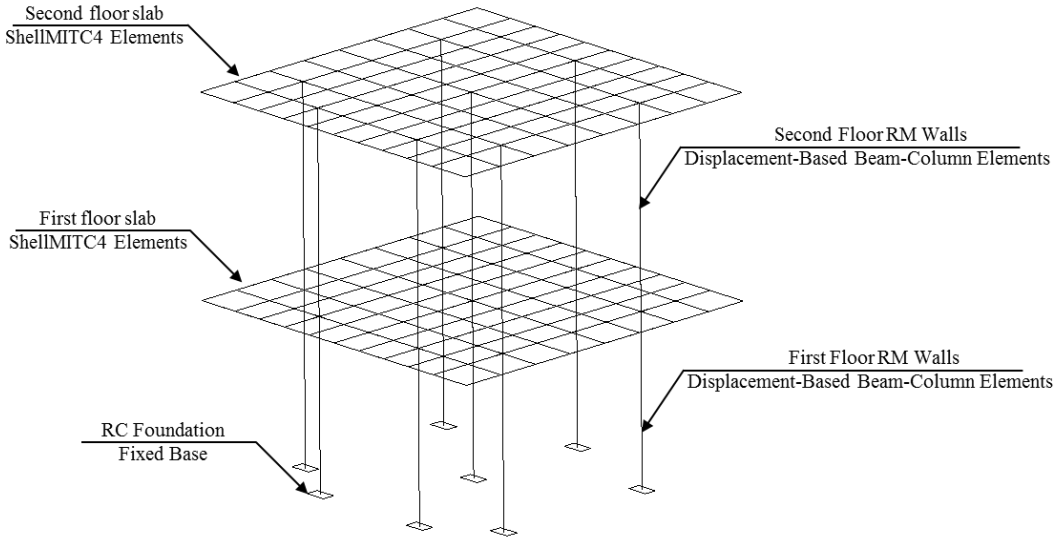

Figure 4: Schematic diagram of the 3D model.

4.2 Material Model

Chang and Mander's model for concrete (Concrete07) in OpenSees was used to model the masonry in this work. The Chang and Mander concrete model in OpenSees depends on the compressive strength, f'_m, the strain at the maximum compressive strength, ε_m, the elastic modulus, E_m, and other parameters that define strength and stiffness degradation. The strength and stiffness degradation parameters were taken according to the formulae reported in Chang et al. (1994). Unlike rectangular RM shear walls in *Building II*, RM walls with boundary elements in *Building IV* have stirrups to confine the masonry and the vertical reinforcement near the extreme compression fiber. This confinement significantly enhances both the strength and the ductility of the compressed masonry zone (boundary element region). This was taken into consideration by assigning different material properties for the masonry inside the closed ties at the boundary element area, as shown in Figure 3b. The model by Mander et al. (1988) was used to calculate the compressive strength, f'_{mc}, and the strain at maximum compressive strength, ε_{mc}, within the boundary element confined area as shown in Equations 1 and 2:

[1] $f'_{mc} = f'_m(1+x')$

[2] $\varepsilon_{mc} = \varepsilon_m(1+k_2x')$

where k_1, k_2 and x' are factors that depend on the vertical and horizontal reinforcement ratios in the boundary elements. The reinforcement steel was modelled using a Giuffre-Menegotto-Pinto model (Steel02). This model is defined by the yield strength, initial elastic modulus, post-yield tangent modulus and other constants that control the transition from elastic to plastic zone. All of these properties and parameters were defined based on material characterization tests as shown in Table 1, without any need for calibration to the overall wall response. This approach has previously been validated against experimental results for individual walls by Ezzeldin et al. (2015).

5. COMPARISON BETWEEN NUMERICAL AND EXPERIMENTAL RESULTS

Figure 5 shows that there is good agreement between the experimental hysteresis loops and the corresponding loops from the cyclic analysis using OpenSees. The models are able to simulate most relevant characteristics of the buildings' cyclic response, including the initial stiffness, peak load, stiffness degradation, strength deterioration, hysteretic shape and pinching behaviour at different drift levels. The following sections discuss these parameters in more detail.

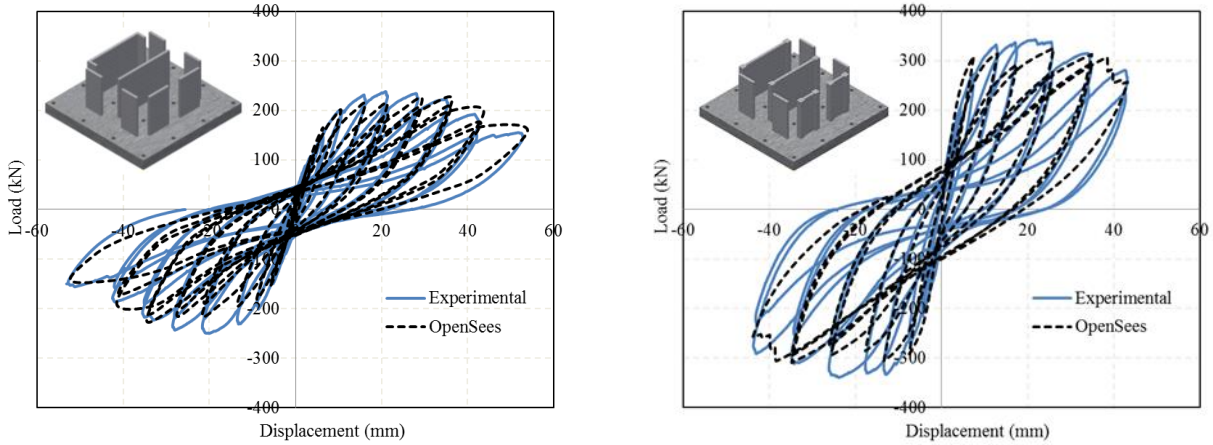

(a) *Building II*. (b) *Building IV*.

Figure 5: Experimental and numerical hysteresis loops of *Building II* and *Building IV*.

5.1 Hysteretic Behaviour

Figure 6 compares the individual the experimental and numerical hysteresis loops for *Building II*, using the first cycle at each drift level. The figure shows that the model can capture the loading and unloading stiffness, as well as the pinching behaviour. These ranges cover almost the entire portion of the load-displacement curve up to 80% strength degradation. Similar results were obtained for *Building IV*, but graphs are not shown here.

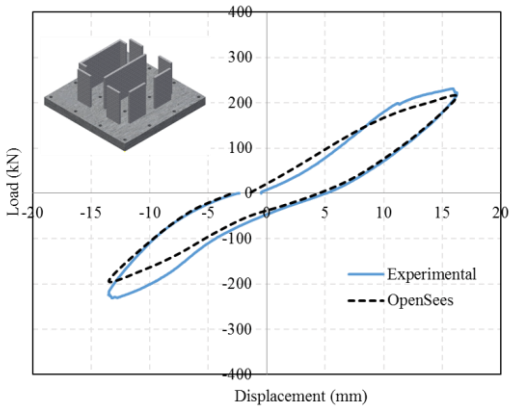

(a) At Drift = 0.70 %

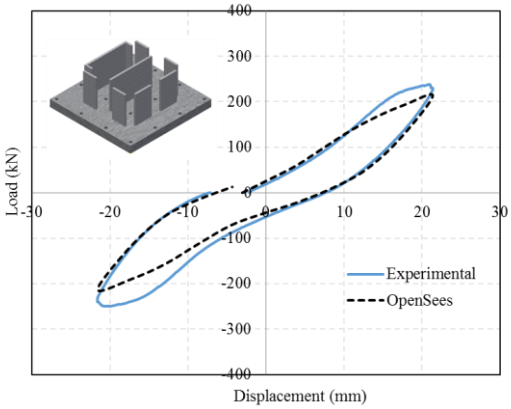

(b) At Drift = 1.00 %

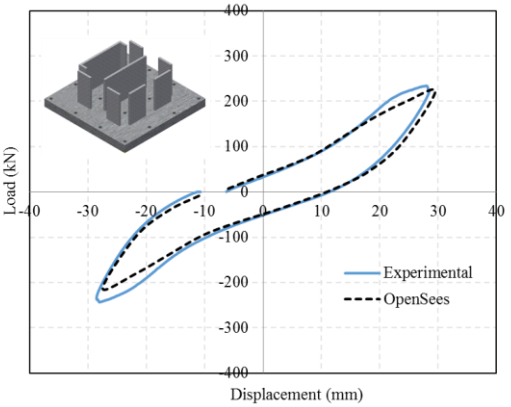

(c) At Drift = 1.40 %

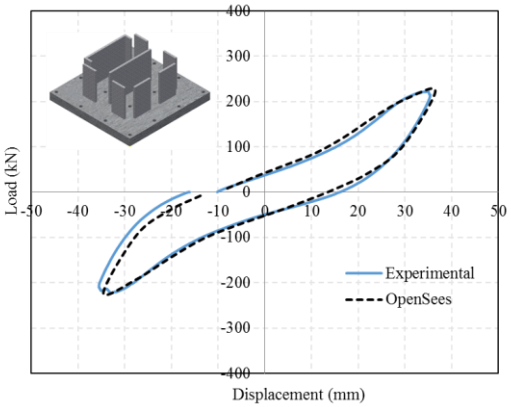

(d) At Drift = 1.70 %

Figure 6: Detailed experimental and numerical hysteresis loops of *Building II*.

5.2 Lateral Capacity

The lateral capacities of *Building II* and *Building IV* were represented very accurately for most of the lateral drift levels, as shown in Figure 7. Relative to the experimental results, the maximum percentage of error in the lateral load either in push or pull directions is less than 13 % and 14 % in *Building II* and *Building IV*, respectively.

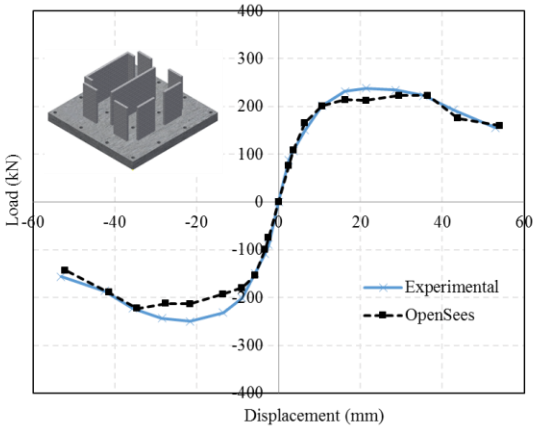

(a) *Building II*.

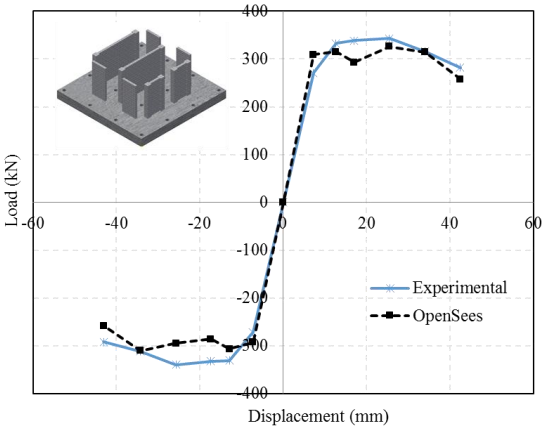

(b) *Building IV*.

Figure 7: Lateral experimental and numerical load envelopes of *Building II* and *Building IV*.

5.3 Energy Dissipation

Energy dissipation through hysteretic damping, E_d, is an important aspect in seismic design because it reduces the amplitude of the seismic response. Previous research showed that the envelope of the load-displacement hysteresis loops is relatively insensitive to the imposed displacement increments and to the number of cycles (Hose and Seible 1999). Therefore, the energy dissipation, E_d, is represented by the area enclosed by the load-displacement curve passing through the envelope values at each displacement level, as suggested by Hose and Seible (1999). Figure 8 shows that the energy dissipation increased significantly at higher drift levels. Although the OpenSees model systematically underestimates the energy dissipated, the difference between the experimental and numerical results is less than 14% and 12% for *Building II* and *Building IV*, respectively.

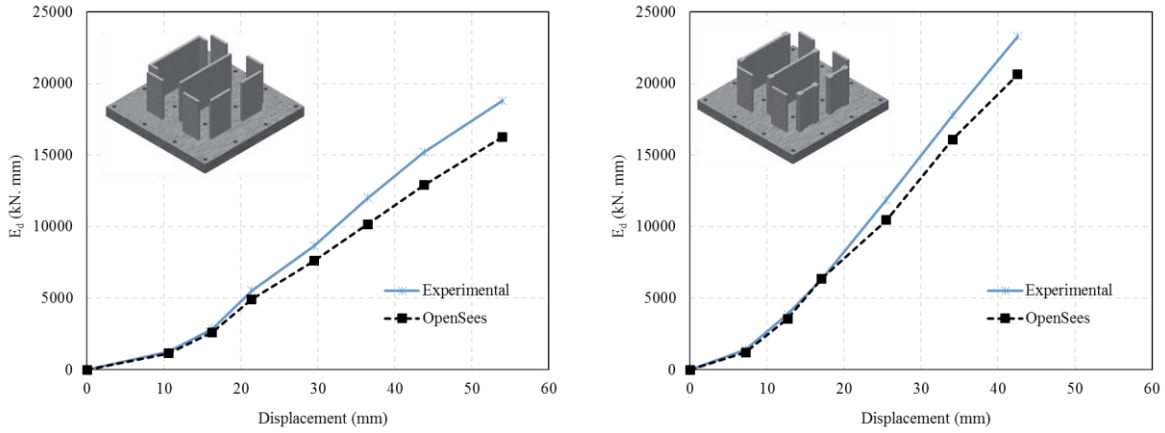

(a) *Building II*. (b) *Building IV*.

Figure 8: Experimental and numerical energy dissipation of *Building II* and *Building IV*.

6. CONCLUSIONS

This paper developed a 3D numerical macro model using OpenSees to simulate the cyclic behaviour of reinforced masonry shear wall buildings with different wall configurations and slab details. Data from two experimental test programs were used to verify the proposed modelling technique, and it was found that this model is generally able to capture the peak values of cyclic load that were measured in the experiments, as well as the hysteretic behaviour and the energy dissipation. This paper demonstrated that reinforced masonry shear walls buildings can be simulated accurately using a simple macro model scale.

The analyses in this paper were limited to two particular RM shear wall buildings, one with traditional shear walls and with the slab specially detailed to avoid coupling between these walls, and the other without special slab detailing but with boundary elements as part of the walls in the loading direction. Further experimental data would be needed to validate this approach for other wall systems, such as walls with openings. In addition, the reliability of the numerical model was shown to depend on the assumed plastic hinge length. Ongoing research seeks to verify the robustness of the model for different buildings with different wall aspect ratios. Research is also underway to apply this modelling technique to understand the inelastic dynamic behaviour of reinforced concrete masonry block shear walls buildings under seismic loads.

ACKNOWLEDGMENTS

The financial support for this project was provided through the Natural Sciences and Engineering Research Council (NSERC) of Canada. Support was also provided by the McMaster University Centre for Effective Design of Structures (CEDS), funded through the Ontario Research and Development Challenge Fund (ORDCF) of the Ministry of Research and Innovation (MRI) as well as the Canada Masonry Design Centre (CMDC).

NOTATION

C_M	=	Building floor center of mass;
C_R	=	Building center of rigidity;
E_d	=	Energy dissipation;
E_m	=	Masonry Young's modulus;
f'_m	=	Masonry compressive strength;
f'_{mc}	=	Masonry compressive strength within the boundary elements area;
ε_m	=	Masonry strain at maximum compressive strength;
ε_{mc}	=	Masonry strain at maximum compressive strength within the boundary elements area.

REFERENCES

Ashour, A., Shedid, M. and El-Dakhakhni, W. 2015. Slab Rigidity Effects on Reinforced Masonry Building Behavior. *12th North American Masonry Conference*, Denver, Co, USA, 12 p. paper in CD-ROM proceedings.

Bohl, A. and Adebar, P. 2011. Plastic Hinge Lengths in High-Rise Concrete Shear Walls. *American Concrete Institute Structural Journal*, 108(2): 148-157.

Chang, G.A. and Mander, J.B. 1994. Seismic Energy Based Fatigue Damage Analysis of Bridge Columns: Part 1– Evaluation of Seismic Capacity. *NCEER Technical Report No. NCEER-94-0006*, State University of New York, Buffalo, N.Y, 164 Pages.

Coleman, J. and Spacone, E. 2001. Localization Issues in Forced-Based Frame Elements. *Journal of Structural Engineering*, 127(11): 1257-1265.

Ezzeldin, M., Wiebe, L., Shedid, M. and El-Dakhakhni, W. 2014. Numerical Modelling of Reinforced Concrete Block Structural Walls Under Seismic Loading. *9th International masonry conference*, Guimarães, Portugal, 12 p. paper in CD-ROM proceedings.

Ezzeldin, M., Wiebe, L. and El-Dakhakhni, W. 2015. Numerical Modelling of Reinforced Concrete Block Structural Walls with Boundary Elements Under Seismic Loading. *11th Canadian conference on Earthquake Engineering*, Victoria, Canada, 10 p. paper in CD-ROM proceedings.

Ezzeldin, M., El-Dakhakhni, W. and Wiebe, L. 2016. System-Level Seismic Performance Assessment of an Asymmetrical Reinforced Concrete Block Building with Boundary Elements. *16th International Brick and Block Masonry conference*, Padova, Italy.

Guinea, G.V., Hussein, G., Elices, M. and Planas, J. 2000. Micromechanical Modelling of Brick-Masonry Fracture. *Cement Concrete Research*, 30: 731–737.

Heerema, P., Ashour, A., Shedid, M. and El-Dakhakhni, W. 2015. System-Level Displacement and Performance-Based Seismic Design Parameter Quantifications for an Asymmetrical Reinforced Concrete Masonry Building. *Journal of Structural Engineering*, 10.1061/ (ASCE) ST.1943- 541X.0001258 04015032.

Hose, Y. and Seible, F. 1999. Performance Evaluation Database for Concrete Bridge Components and Systems under Simulated Seismic Loads. *PEER report. Berkley (USA)*, Pacific Earthquake Engineering Research Center, College of Engineering, University of California.

Legeron, F., Paultre, P. and Mazars, J. 2005. Damage Mechanics Modeling of Nonlinear Seismic Behavior of Concrete Structures. *Journal of Structural Engineering*, (131)6: 946-955.

Lourenço, P. and Rots, J. 1997. Multisurface Interface Model for Analysis of Masonry Structure. Journal of Engineering Mechanics, 123(7): 660-668.

Lu, X., Xie, L., Guan, H., Huang, Y. and Lu, X., 2015. A Shear Wall Element for Nonlinear Seismic Analysis of Super-Tall Buildings using Opensees. *Finite Elements in Analysis and Design*, 98: 14-25.

McKenna, F., Fenves, GL. and Scott, MH. 2013. Open System for Earthquake Engineering Simulation, University of California, Berkeley, CA, 2000. Available from: *http://opensees.berkeley.edu*, Version 2.4.6.

Mander, J. B., Priestley, M. J. N. and Park, R. 1988. Theoretical Stress-Strain Model for Confined Concrete. *Journal of Structural Engineering*, 114(8): 1804–1826.

Stavridis, A. and Shing, P. B. 2010. Finite-Element Modeling of Nonlinear Behavior of Masonry-Infilled RC Frames. *Journal of Structural Engineering*, (136)3: 285-296.